

Sc substitution for Mg in MgB_2 : effects on T_c and Kohn anomaly

S. Agrestini, C. Metallo, M. Filippi, L. Simonelli, G. Campi, C. Sanipoli

Dipartimento di Fisica, Università di Roma "La Sapienza", P.le Aldo Moro 2, 00185 Roma, Italy

E. Liarokapis

Department of Applied Mathematics and Physics,
National Technical University of Athens, GR-157 80 Athens, Greece

S. De Negri, M. Giovannini, A. Saccone

Dipartimento di Chimica e Chimica Industriale, Università di Genova, Via Dodecaneso 31, 16146 Genova, Italy

A. Latini

Dipartimento di Chimica, Università di Roma "La Sapienza", P.le Aldo Moro 2, 00185 Roma, Italy

A. Bianconi

Unità INFN and Dipartimento di Fisica, Università di Roma "La Sapienza", P.le Aldo Moro 2, 00185 Roma, Italy

(dated: March 22, 2024)

Here we report synthesis and characterization of $\text{Mg}_{1-x}\text{Sc}_x\text{B}_2$ ($0.12 < x < 0.27$) system, with critical temperature in the range of $30 > T_c > 6$ K. We find that the Sc doping moves the chemical potential through the 2D/3D electronic topological transition (ETT) in the band where the "shape resonance" of interband pairing occurs. In the 3D regime beyond the ETT we observe a hardening of the E_{2g} Raman mode with a significant line-width narrowing due to suppression of the Kohn anomaly over the range $0 < q < 2k_F$.

PACS numbers: 74.70Ad; 74.62Dh; 78.30.-j

Following the discovery of superconductivity in MgB_2 with a T_c of 40 K large attention has been paid to chemical substitutions^{2,3,4,5,6,7,8} aiming at enhancement of T_c and H_{c2} , and to manipulate the electronic structure for the understanding of the high T_c superconductivity. As a matter of fact, chemical substitution in the MgB_2 is difficult and only Al replacing Mg^{4,5,6,7} and C replacing B⁸ had been successful. Both of these substitutions reduce the T_c and induce a lattice compression. The variation of T_c with doping is mostly determined by the tuning of the chemical potential through the electronic topological transition (ETT) where the topology of the Fermi surface of the band changes from 2D to 3D⁶. In this two-gap superconductor⁹ the exchange-like non-diagonal - interband pairing terms that enhance T_c are expected to exhibit large variation near the ETT^{5,6}. In addition, Raman spectroscopy measurements on the $\text{Mg}_{1-x}\text{Al}_x\text{B}_2$ and $\text{MgB}_{2-x}\text{C}_x$ systems^{10,11,12,13} have revealed a line-width narrowing and energy hardening of the E_{2g} mode with the substitution beyond the ETT. This effect could be interpreted in terms of suppression of the Kohn anomaly^{14,15} observed over an extended range $0 < q < 2k_F$ in the MgB_2 ^{16,17} by a shift of the Fermi level. In fact the Kohn anomaly¹⁸ is strong (weak) for a 2D (3D) Fermi surface^{19,20}. Therefore it is expected to decrease for a 2D to 3D ETT^{6,20} of the Fermi surface. The proximity to an ETT has been invoked to explain the anomalous pressure dependence²² of this mode and it has been proposed to be the driving mechanism for raising the critical temperature^{6,23,24}. The aim of this work is to modify the band structure by chemical substitutions

to explore the role of electronic structure in the MgB_2 on the electron-phonon coupling and on T_c by tuning the chemical potential through the shape resonance.

We have synthesized the new superconducting ternary system $\text{Mg}_{1-x}\text{Sc}_x\text{B}_2$ for $0.12 < x < 0.27$, where the chemical substitution induces minor lattice variations since the ionic radius of Sc (1.62 Å) is only a little larger than of Mg (1.602 Å). The substituted Sc ions donate $0.12 < x < 0.27$ electrons per unit cell to the conduction bands so the chemical potential is shifted towards the top of the band beyond the ETT⁶ where the Fermi surface changes from a 2D to a 3D topology, expected near $x = 0.12$ ^{9,18}. Sc substitution for Mg increases the disorder in the Mg/Sc layers but has minor effects on the lattice structure of the boron layer. Therefore the variation of T_c and electron-phonon coupling with the variation of the electron structure can be well investigated.

In these new samples we observe a remarkable line narrowing and frequency hardening of the E_{2g} Raman mode, which gives a compelling experimental evidence for a drastic reduction of the Kohn anomaly and of the electron-phonon coupling for $x > 0.12$. It is remarkable to note that the critical temperature in the $\text{Mg}_{1-x}\text{Sc}_x\text{B}_2$ samples has been dropped only by a factor 2-10 from MgB_2 , much less than expected for a multiband theory (with doping-independent interband pairing) considering the decrease of the electron-phonon coupling and of the density of states in the band. This suggests importance of the resonant enhancement of the interband pairing term²³ and the associated minimum of the non-diagonal Coulomb pseudo-potential²⁴ that drives the T_c .

amplification at the ETT, called "shape resonance" in a two-gap superconductor.

$Mg_{1-x}Sc_xB_2$ samples were synthesized by direct reaction method of the elemental magnesium and scandium (powder, 99.9 mass % nominal purity), boron (99.5 % pure < 60 mesh powder). The starting materials were mixed in a stoichiometric ratio and pressed into pellets of 8 mm in diameter. Each pellet was enclosed in a tantalum crucible and sealed by arc welding under argon atmosphere. The Ta crucibles were then heated in a furnace Centorr M 60 under high-pure Ar atmosphere for 14 hours in the temperature range between 1280 and 950 °C.

The phase purity of the samples was checked by X-ray diffraction. The diffraction patterns of $Mg_xSc_xB_2$ samples were measured in the Bragg-Brentano geometry by a vertical X'Pert Pro MPD diffractometer using a Cu K α radiation. The X-ray diffraction measurements of several samples were repeated at the beam line ID 31 of the European Synchrotron Radiation Facility (ESRF), Grenoble. The samples were sealed in 1.0 mm diameter glass capillaries and the high-resolution diffraction profiles ($\lambda = 0.5 \text{ \AA}$) were collected at $T = 80 \text{ K}$ using nine Ge(111) analyzer crystals. The reflections were indexed to a MgB_2 -like structure according to the hexagonal AB_2 structure type (P6/mmm space group). No Sc, Sc_2O_3 or ScB_{12} minority phases were found, which indicates a successful Sc substitution for Mg. Figure 1a shows profiles of (002) and (110) diffraction peaks for representative sample of the $Mg_{1-x}Sc_xB_2$ system. A line broadening is observed in Sc-doped compounds as compared to MgB_2 and ScB_2 indicating disorder or non-uniformities due to Mg/Sc layers.

The samples were characterized for their superconducting properties by the temperature dependence of complex conductivity using the single-coil inductance method^{5,6}. The temperature dependent radio-frequency complex conductivity for representative Sc contents is shown in Fig. 1b where it can be seen that the introduction of Sc in the Mg-planes induces a clear shift of the superconducting transition to lower temperatures. The superconducting transition for the Sc-doped samples shows a broadening. This indicates that some disorder does exist in the Sc-doped samples with possible effect on the superconductivity via an increase of intraband scattering in the band.

The Raman spectra were measured in the back-scattering geometry, using a T64000 Jobin-Yvon triple spectrometer with a charge-coupled device camera. The explored Raman shift ranges between 200 and 1100 cm^{-1} . The 488.0 nm Ar⁺ laser line was focused on 1-2 μm large crystallites and the power was kept below 0.03 mW to avoid heating by the beam. Typical spectra recorded for selected temperatures are shown in Fig. 1c. The in-plane Boron vibration with E_{2g} symmetry produces a single narrow peak in Raman spectrum of ScB_2 as in AlB_2 ^{10,12} also if at lower energy according with its larger lattice parameters. The Raman line is softened going from ScB_2

to $Mg_{1-x}Sc_xB_2$ and finally becomes very soft and very broad in MgB_2 .

The diffraction data were analyzed by Rietveld refinement using GSAAS program. The behaviour of the lattice parameters a and c as a function of Sc content is reported in Fig. 2. A miscibility gap occurs in the range from 2 % to 12 % Sc substitution where the samples show a macroscopic phase separation between low-doped and high-doped samples. The a -axis increases gradually with increasing Sc-content, while the c -axis is nearly constant. The unit cell volume shows a small expansion in agreement with the similar ionic radius between Sc^{3+} and Mg^{2+} . For comparison in the same figure we report the evolution of the lattice parameters in the $Mg_{1-x}Al_xB_2$ system that shows much larger lattice variations. Here " x " is the nominal Sc-content and we can conclude that the introduced Sc is successfully substituted for Mg, and the actual Sc-content is not much different from the nominal value. From the variation of lattice parameters with Sc content, we can conclude that the solubility range of Scandium in MgB_2 is between 12% and 27%.

The variation of the superconducting critical temperature T_c as a function of Sc doping is reported in the panel (a) of Fig. 3. The transition temperature T_c was determined from the peak in derivative of the complex conductivity. The T_c decreases continuously with increasing Sc substitution from 30K at 12% to 6K at 27%. It is interesting to note that the variation of $T_c(x)$ is sharper for $0.12 < x < 0.15$.

The panel (b) of Fig. 3 shows the variation of the frequency of the E_{2g} Raman line from MgB_2 to $Mg_{1-x}Sc_xB_2$. The error bars indicate the E_{2g} peak halfwidth. In the Sc-substituted samples in the range 12% -27% the phonon peak is shifted toward higher frequency, it is much narrower in comparison with MgB_2 and it is approaching the frequency of that for the ScB_2 . The frequency hardening and the line-width narrowing of the Raman E_{2g} mode indicates a clear decrease of the electron-phonon coupling going from MgB_2 to the Sc-doped samples.

Finally in Fig. 4 we report the energy of the Raman E_{2g} mode as a function of the a -axis (that is the relevant parameter for the in plane high frequency longitudinal optical mode E_{2g}) of the non-superconducting diborides ScB_2 and AlB_2 , and of the superconducting MgB_2 , $Mg_{1-x}Sc_xB_2$ and $Mg_{0.5}Al_{0.5}B_2$ ¹³ systems.

Let us consider first the AlB_2 and ScB_2 samples with a filled band. The energy of the E_{2g} mode as a function of a -axis follows the law $\omega(a) = \omega_0(a/a_0)^{-3}$ (dashed line in panel a) where ω_0 is the Gruneisen parameter $\omega_0 = \partial \ln \omega / \partial \ln a = 1.4 \pm 0.1$ that is the expected behaviour due to lattice expansion for a metallic covalent material.

In the case where the Fermi level is tuned below the top of the band (e.g. MgB_2 , $Mg_{1-x}Sc_xB_2$ and $Mg_{0.5}Al_{0.5}B_2$) a phonon decay channel opens up unlike others with filled band (e.g. AlB_2 and ScB_2). In fact the phonons can now decay into electron-hole exci-

- ¹⁶ A . Shukla, M . Calandra, M . d'A stuto, M . Lazzeri, F . Mauri, C . Bellin, M . K risch, J . K arpinski, S . M . Kazakov, J . Jun, D . D aghero, and K . P arlinski, Phys. Rev. Lett. 90, 095506 (2003).
- ¹⁷ A . Q . R . Baron, H . U chiya m a, Y . Tanaka, S . T sutsui, D . Ishikawa, S . Lee, R . Heid, K . P . Bohnen, S . Tajim a, T . Ishikawa, cond-m at/0309123 (2003).
- ¹⁸ W . E . P ickett, B razilian Journal of Physics 33, 695 (2003); J . M . A n, S . Y . Savrasov, H . Rosner, and W . E . P ickett, Phys. Rev. B 66, 220502-R (2002); W . E . P ickett, J . M . A n, H . Rosner, and S . Y . Savrasov, Physica C 387, 117 (2003) and references therein.
- ¹⁹ S . T suda, T . Yokoya, Y . Takano, H . K ito, A . M atsushita, F . Y in, J . Itoh, H . H arim a, and S . Shin, Phys. Rev. Lett. 91, 12700 (2003).
- ²⁰ A . Carrington, P . J . M eeson, J . R . C ooper, L . B alicas, N . E . Hussey, E . A . Y elland, S . Lee, A . Y am am oto, S . Tajim a, S . M . K azakov, and J . K arpinski, Phys. Rev. Lett. 91, 037003 (2003).
- ²¹ I . M . L ifshitz, Soviet Physics JEPT 11, 1130 (1960).
- ²² A . F . G oncharov, V . V . Struzhkin, Physica C 385 117 (2003).
- ²³ A . B ussm ann-H older and A . B ianconi, Phys. Rev. B 67, 132509 (2003).
- ²⁴ G . A . U mm arino, R . S . G onnelli, S . M assida, A . B ianconi, Physica C 407 121 (2004).
- ²⁵ A . B ianconi, A . V alletta, A . P erali and N . L . Saini, Physica C 296, 269 (1998).

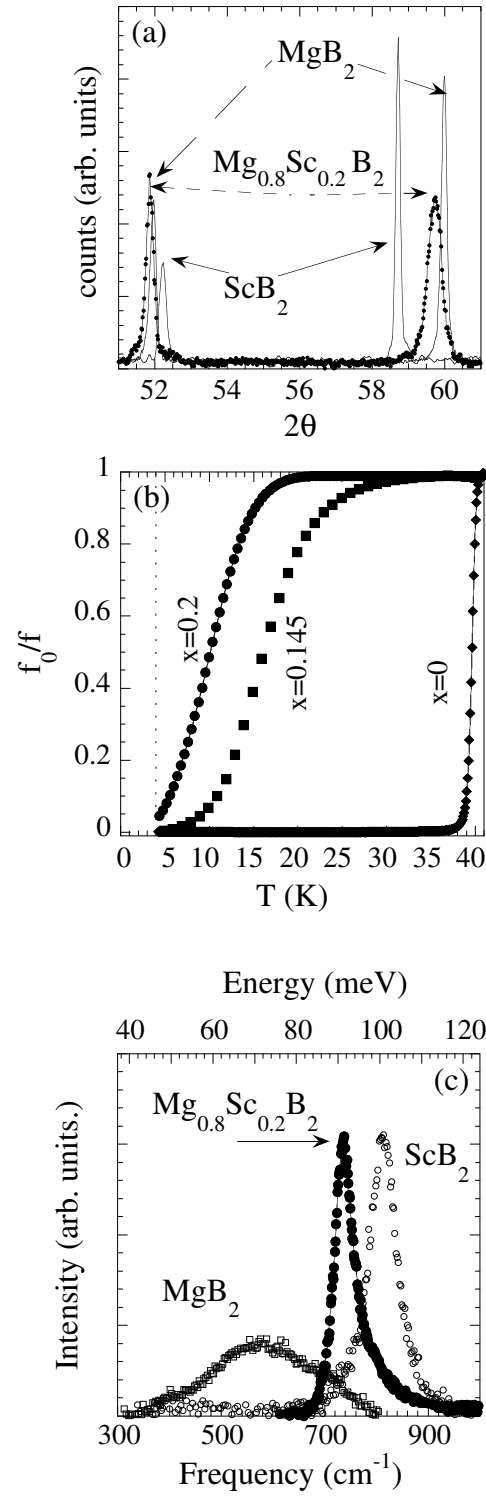


FIG. 1: The X-ray diffraction patterns in the range of the (001) and (110) reflections (panel a), the superconducting transition measured by complex resistivity (panel b), and the Raman spectra (panel c) are shown for representative $\text{Mg}_{1-x}\text{Sc}_x\text{B}_2$ samples compared with MgB_2 and ScB_2 .

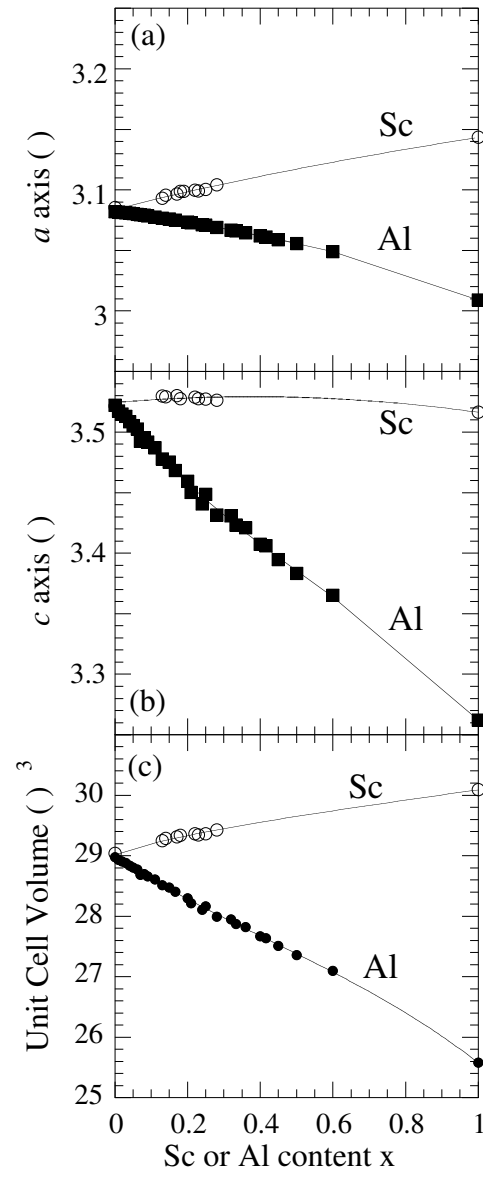


FIG. 2: Changes of lattice parameters a (panel a) and c (panel b) and of unit cell volume v (panel c) as a function of Sc content x in $Mg_{1-x}Sc_xB_2$.

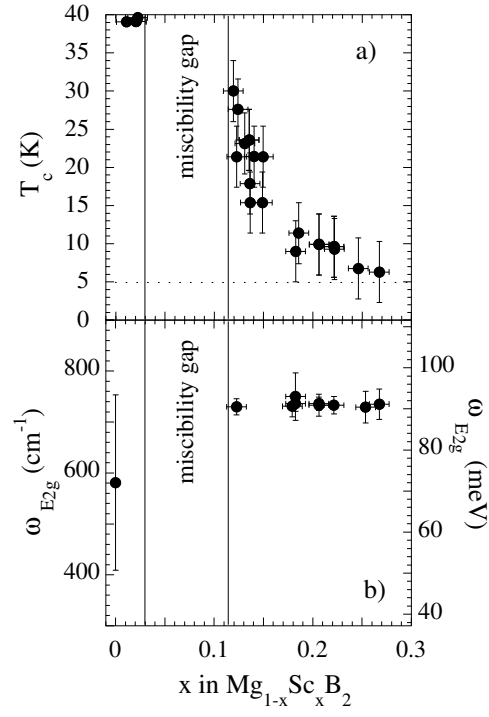


FIG. 3: Evolution of the superconducting critical temperature T_c (panel a), the frequency $\omega_{E_{2g}}$ (panel b) of the E_{2g} Raman line as a function of x in $\text{Mg}_{1-x}\text{Sc}_x\text{B}_2$. The superconductive transition width and the E_{2g} peak halfwidth are indicated as error bars respectively in panel a and panel b.

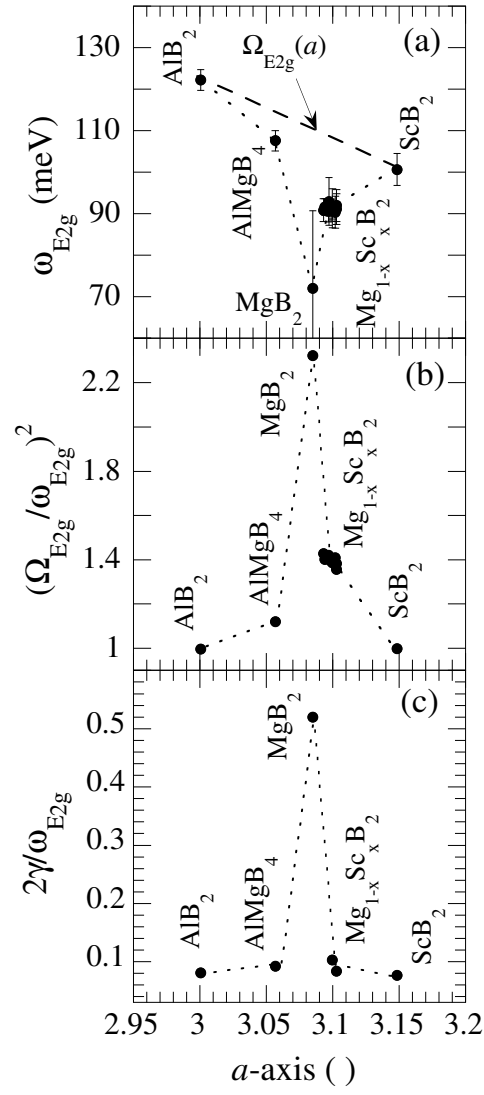


FIG . 4: Variation of the frequency of the E_{2g} Raman line as function of the lattice parameter a for different diborides (panel a). The softening and broadening of the E_{2g} mode due to the Kohn anomaly is given by the energy ratio $(\Omega_{\text{E}_{2g}}/\omega_{\text{E}_{2g}})^2$ (panel b) and the ratio $2\gamma/\omega_{\text{E}_{2g}}$ (panel c) where 2γ is the Raman line-width.